Lead Oxide Nanodots Synthesized by Solvothermal and Microwave Assisted Method and its Comparative Characterization

MOHD KASHIF AZIZ[1,*], , ABUL KALAM[2], , GHULAM MUSTAFA[1], , SHEKHAR SRIVASTAVA[1], and SYED KASHIF ALI[3],

[1]Department of Chemistry, University of Allahabad, Prayagraj-211002, India
[2]Department of Chemistry, College of Science, King Khalid University, P.O. Box 9004, Abha 61413, Saudi Arabia
[3]Department of Chemistry, Faculty of Science, Jazan University, P.O. Box 114, Jazan, Saudi Arabia

*Corresponding author: E-mail: mohdkashifaziz@allduniv.ac.in

This study is focused on synthesis of lead oxide (PbO) nanodots (quantum dots) *via* two methods *viz*. microwave-assisted (B) and solvothermal method (A). The results of microwave-assisted method are slightly different in comparison to the solvothermal method. Several techniques, such as Fourier transform infrared spectroscopy (FTIR), ultraviolet-visible spectroscopy (UV-Vis), powder X-ray diffraction (XRD), transmission electron microscopy (TEM) and selective area electron diffraction (SAED) were used for characterizing PbO nanodots synthesized by both methods. The FTIR peak at 687 cm^{-1} indicated the formation of the Pb-O-Pb bond. The band gap, calculated with the help of UV data, was ~5.5 eV. The obtained PXRD pattern and miller indices suggested the formation of β-PbO and α-PbO nanoparticles with orthorhombic and tetragonal geometries. The crystallinity of PbO nanodots methods by A and B methods was 96% and 99%, respectively. The average crystallite size (for both samples synthesized by methods A and B) calculated by Debye-Scherrer's equation was 42 and 38 nm, respectively. Sample A mostly contains α-type lead oxide nanodots, while sample B mainly contains mostly β-type lead oxide nanodots. The average size of nanodots observed from TEM images for samples A and B was 3.7 and 2.7 nm, respectively.

Keywords: Lead oxide, Nanoparticles, Microwave, Crystallinity, Nanodots, Nanoplates.

INTRODUCTION

Nanotechnology comprises of the control synthesis, manipulation and study of nanoscale materials whose sizes are less than 100 nm [1]. It is an interdisciplinary field that enables the progression of novel fascinating, materials with valuable features [2]. In 1959, Nobel laureate Richard Phillips Feynman at the American Physical Society meeting lectured on the title "There's Plenty of Room at the Bottom: An Invitation to Enter a New Field of Physics", where he considered a further prominent "form of synthetic chemistry than those used earlier" [3]. According to him, there is a vast potential for the physicist to work at nanometer scale, if not angstrom. Nanoparticle's properties are novel and can be modulated *via* chemical, biological or physical processes [4]. Magnetic, electronic, antibacterial, catalytic and optical properties of metal oxide nanoparticles depends upon their shape, size and chemical composition [5-9]. Technology is not new to the world, it was also present in an ancient era, just it got the term nano in recent decades. Approxi-

mately 4000 years ago, lead-based cosmetics were invented in ancient Egypt [10]. Researchers are inquisitive about lead oxide nanoparticles, as observed by an increase in the number of research publications in previous decades. However, lead oxide nanoparticles are found to be carcinogenic in nature. Lead oxide nanoparticles have inimitable physico-chemical properties, like high surface atom fraction and specific surface area, which endure a significant transformation in the field of research.

There different types of oxides of lead, which include PbO, Pb_2O_3, Pb_3O_4 and PbO_2. Among all the oxides of lead, mostly PbO is studied and α, β and amorphous structure are exhibited by PbO_2. Lead oxide nanoparticles have exceptional properties and vast applications such as gas sensors [11], storage devices [12,13], luminescent resources [11], batteries [14], pigments & paints [15], ceramics [16], as a catalyst in synthetic organic chemistry, nanomedicines [17] UV-blockers and as a modernizer in glasses [18]. It is becoming increasingly common to use nanomaterials for commercial purposes [19,20]. Inorganic

nanomaterials like quantum dots, nanorods and nanowires having optical and electrical properties make them suitable for optoelectronic applications. Materials comprised of metals, semiconductors or oxides have enormous mechanical, magnetic, chemical and other properties [21,22]. In addition, nanoparticles are used in the formation of quantum dots and chemical catalysts, such as those based on nanomaterials. Nanoparticles have biomedical applications like tissue engineering and biosensors, medication delivery as examined in recent studies [23,24].

There are several ways to synthesized lead oxide nanoparticles, but the chemical process is particularly effective at altering the shape and size of the end product. Owing to the different types of morphology lead oxide nanoparticles show an essential role in properties. It may come into view in several forms like nanostars, nanodendrites [25], nanoplates, nanorods [26], nanosheets and nanotubes [27] and nanopowders [28]. α-PbO has a tetragonal crystal with red colour called litharge, stable at room temperature though β-PbO has a orthorhombic crystal that shows a yellow colour called as massicot, stable at high temperature, more than 489 ºC [29].

Nanosize lead oxide is produced by various physico-chemical methodologies, including spray pyrolysis, selected control synthesis, sonochemical, microwave irradiation synthesis, pulsed current electrochemical methods and thermal decomposition [30]. Due to their ease of synthesis, low cost and quick turnaround time, lead oxide nanodots are the focus of the current investigation *i.e.* solvothermal and microwave irradiation. The characterization of the synthesized nanodots was confirmed by FTIR, UV-vis spectroscopy, XRD and TEM techniques.

EXPERIMENTAL

Synthesis of lead oxide nanodots: In the following experiment, lead acetate trihydrate [Pb(CH₃COO₂)₂·3H₂O] has been used as precursor for the formation of lead oxide nanodots *via* solvothermal method. A solution of 0.5 M lead acetate trihydrate was prepared in 250 mL volumetric flask by adding warm double distilled water with continuous stirring at a temperature up to 70 ºC for 20 min. Then, 0.5 M laqueous solution of ead acetate was divided into two reactions A and B with equal 70 mL in a round bottom flask, followed by dropwise addition of 40 mL of 5 M NaOH solution.

The round bottom flask A was heated at 90 ºC with continuous stirring. After a while, a white cloudy-clumsy, then reaction mixture turned to yellow and then turned to peach colour and finally a deep orange precipitate has been formed.

In round bottom flask B continuous stirring at room temperature was performed. After a few minutes reaction mixture turned white and then into a yellowish peach colour and at the end bright orange precipitate has been observed.

Slow colour phasing has been observed for round bottom flask B as compared to flask A reactions. After the formation of orange colour precipitate, both flasks were allowed to settle down for about 1 h followed by decantation of supernatant. Then flask B reaction solutions were irradiated with microwave radiation for 45 s. Both reaction flasks A and B were dried in a hot air oven for 10 h at 80 ºC and then samples were removed from the round-bottom flask and grind into powder using a

mortar and pestle. Furthermore, to produce highly crystalline PbO nanodots, samples A and B were calcined for 2 h at 390 ºC in a muffle furnace.

FTIR analysis: Fourier transform infrared (FTIR) spectra of the sample has been recorded on Bruker Alpha instrument with ATR (Attenuated Total Reflection) mode spectrophotometer with a resolution of 2 cm⁻¹ at STP (Standard Temperature and Pressure) in the wavenumber range of 4000-500 cm⁻¹

UV-visible analysis: The UV-visible spectral analysis of samples were performed on ELICO SL-210 double beam spectrophotometer instrument in the 190 to 600 nm wavelength range. The UV-Vis spectral data has been used for evaluation of energy gap according the literature methods [31]. The following formula has been used for calculating the energy gap:

Tauc equation:

$$\alpha h\nu = \alpha \, (h\nu - E_g)^n$$

where α = Absorption coeficient; $h\nu$ = Photon energy; E_g = Energy band gap; n = ½ - direct band gap transition; 2-indirect band gap transition.

PXRD analysis: There structural characterization has also been done for the validation of PbO nanodots. The X-ray diffractometer investigations of the powdered samples were performed on Philips X'pert Model XRD using Cu$K\alpha$ X-rays of wavelength λ = 1.54 Å in the Bragg's angle range 2θ = 10º to 80º.

Powder XRD is a swiftly investigative technique, which is predominantly utilized for phase identification of crystallinity and to find the unit cell dimensions. Normally, Debye-Scherrer's equation has been used for the determination of the average particle size of a PbO nanodots [24].

$$D = \frac{0.9\lambda}{\beta\cos\theta}$$

where D = Crystallite size of the particles; λ = Wavelength of the X-rays; β = FWHM (full-width at half-maximum) of the X-ray diffraction peak in radians; θ = Bragg angle.

TEM analayis: TEM analysis was done to analyze the morphology of the synthesized PbO nanoparticles by FEI-Tecnai-Netherland of model G2F30S-Twin by Schottky field emission gun at voltage 300 kV with a lattice resolution of 0.1 nm.

RESULTS AND DISCUSSION

FTIR studies: The FTIR spectra of samples A and B of PbO nanodots are presented in Fig. 1. The observed results found to be in accordance with the literature values [32]. The peak confinement of PbO nanodots in FTIR spectra confirmed its presence in both samples A and B. The peak at 687 cm⁻¹ was observed for both samples (A and B), which has been attributed to the formation of Pb-O-Pb bond. Due to the emergence of prominent peak at 1398 cm⁻¹ to the –OH stretching, which is also responsible for the Pb-O stretching [29].

UV-VIS studies: The optical properties of PbO nanodots were studied in the range of 200 to 600 nm. In UV-Vis spectra (Fig. 2), the observed broad absorption peak at 250-260 nm confirmed the presence of PbO nanodots.
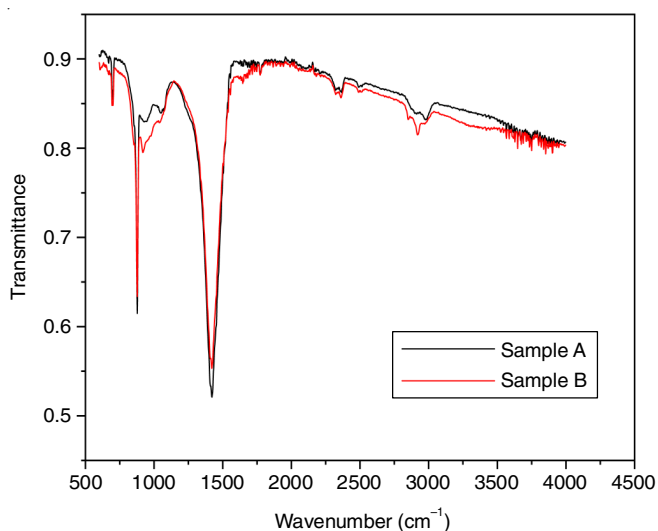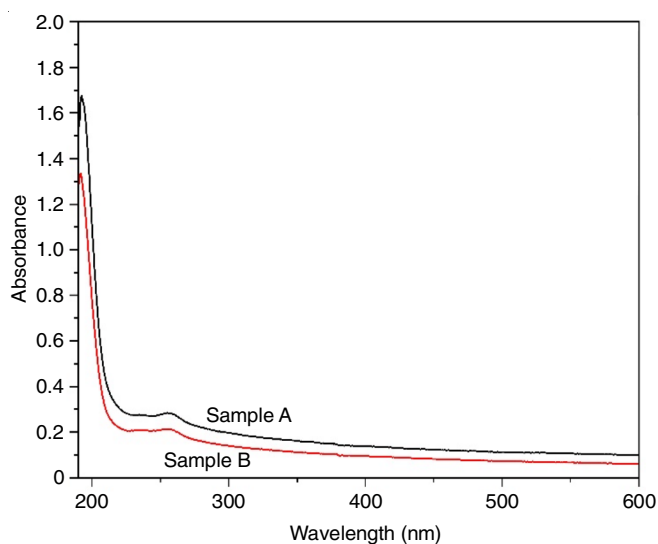
Fig. 1. FTIR spectra (500-4500 cm^{-1}) of samples A and B of PbO nanodots

Fig. 2. UV-Vis spectra (200-600 nm) of samples A and B of PbO nanodots

Fig. 3. Tauc plot for calculation of energy band gap value of both the samples A and B
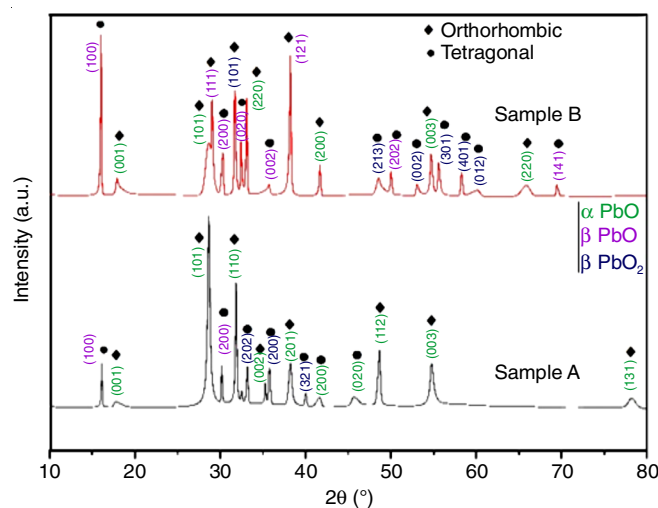
Fig. 4. XRD pattern of lead oxide nanodots for sample A and B

Tauc relation has been used to determine the energy band gap in accordance to reported method [31]. The energy band gap value of PbO nanodots synthesized by method A and B was found to be ~5.5 eV. The Tauc plot has been presented in Fig. 3. Literature also supports the possibility of high energy band gap of 5.52 eV [33]. The observed band gap is very high, which may be due to quantum confinement effect (eqn. 1) since they are the reciprocal of quantitative dependent value R(radius). If the size of the nanoparticle is small then the energy band gap value will also increase.

$$\Delta E_g = E_g^{Nano} - E_g^{Bulk} = h^2 \frac{\pi^2}{2MR^2} \qquad (1)$$

where, R = radius of the nanoparticles and M = mass of the electron.

XRD studies: The powder X-ray diffraction (PXRD) technique was used to investigate the PbO nanodots samples *viz.* sample A and sample B. The XRD pattern (Fig. 4) suggested that the synthesized PbO nanodots were of crystalline nature. According to literature the peaks with Miller indices (100),
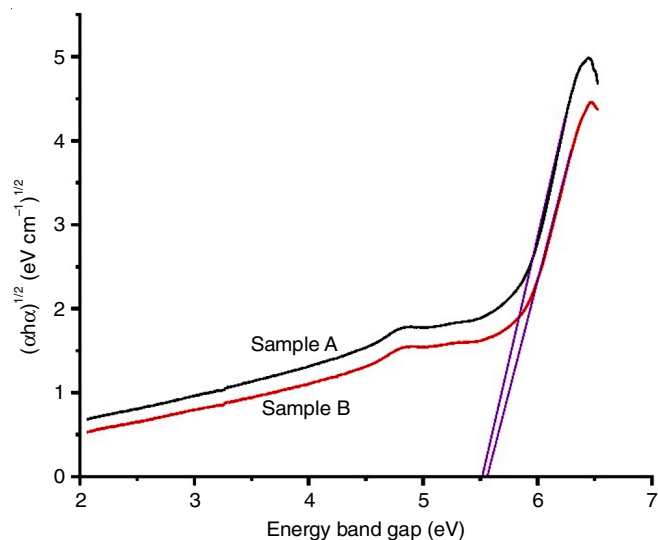
(101), (111), (200), (001), (020), (121), (202), (003), (301), (002), (401), (012), (220), (141), (110), (201), (321), (112) and (131) has been matched for tetragonal and orthorhombic PbO nanodots [25-27]. The obtained PXRD pattern and Miller indices suggested the formation of β-PbO and α-PbO nanoparticles with orthorhombic and tetragonal geometries respectively. The results of PXRD found to be consistent with literature JCPDS data [28].

Along with the regular geometries of β-PbO and α-PbO, the presence of orthorhombic β-PbO$_2$ has also been observed in both samples (calcined at 390 ℃ for 2 h) [27]. The mixed α/β-PbO nanoparticles obtained on calcination at 450-500 ℃ are also reported in the literature [17].

For sample A, the α-PbO nanocrystals was observed, while for sample B, primarily mixed types of α/β-PbO and β-PbO$_2$ nanocrystals were observed. The phase change of α to β PbO nanocrystals was observed at < 390 ℃, which is inferred by PXRD data. The appearances of sharp peaks in the XRD patterns suggested the high crystalline nature of the synthesized nanodots. The average crystallite size for both sample A and

B calculated by Debye-Scherrer's equation were found to be 42 nm and 38 nm, respectively. Both samples A (96%) and B (99%) exhibited a high crystallinity percentage.

Morphology studies: The TEM images of sample A and B along with the size distribution graph are shown in Figs. 5 and 6, respectively. The morphology of samples A and B, as seen in the TEM images, appears to be a nanoplate, but in group, it appears to be nanodots. The average size of the nanoparticle of sample A and B were found to be 3.7 nm and 2.7 nm, respectively.

The SAED patterns of sample A and B are shown in Fig. 7. The spots as well as ring patterns has been observed in SAED pattern suggested the polycrystalline nature of synthesized PbO nanodots. The calculated *d*-spacing of sample A of PbO nanodots were 2.4 Å, 1.73 Å, 1.36 Å, 0.98 Å & 0.88 Å and that for sample B of PbO nanodots was 2.75 Å, 1.81 Å, 1.55 Å, 1.31 Å and 1.01 Å.

Conclusion

Lead oxide (PbO) nanoparticles were synthesized *via* solvothermal (sample A) as well as *via* microwave irradiation (sample B) methods. The colour changing phase during the synthesis confirms the formation of PbO nanodots. The change in phase of α-PbO to β-PbO nanodots occured at < 390 ºC. The β-PbO nanodots were found to be more stable than α-PbO nanodots due to its phase geometry. The synthesized PbO nanodots were also characterized using FTIR & UV-visible spectroscopies. A peak at 687 cm^{-1} indicated the formation of the Pb-O-Pb bond. The calculated band gap using UV data was found to be ~5.5 eV. The obtained PXRD pattern and Miller indices suggested the formation of β-PbO and α-PbO nanodots with orthorhombic and tetragonal geometries. The results have been found to be consistent with literature JCPDS data. The crystallinity of PbO nanodots for sample A and B were found to be 96% and 99%, respectively. Sample A mostly contains α-type PbO nanodots while sample B contains mostly β-type PbO nanodots. The average size of the nanoparticle observed form TEM images for sample A and B have been found to be 3.7 nm and 2.7 nm, respectively. The shape of samples looks like a nanoplate however in group it appeared like nanodots. The synthesized nanodots of lead oxide are of very small size and thus may utilized in many applications such as storage, batteries, solar energies, nanomedicines, *etc.*
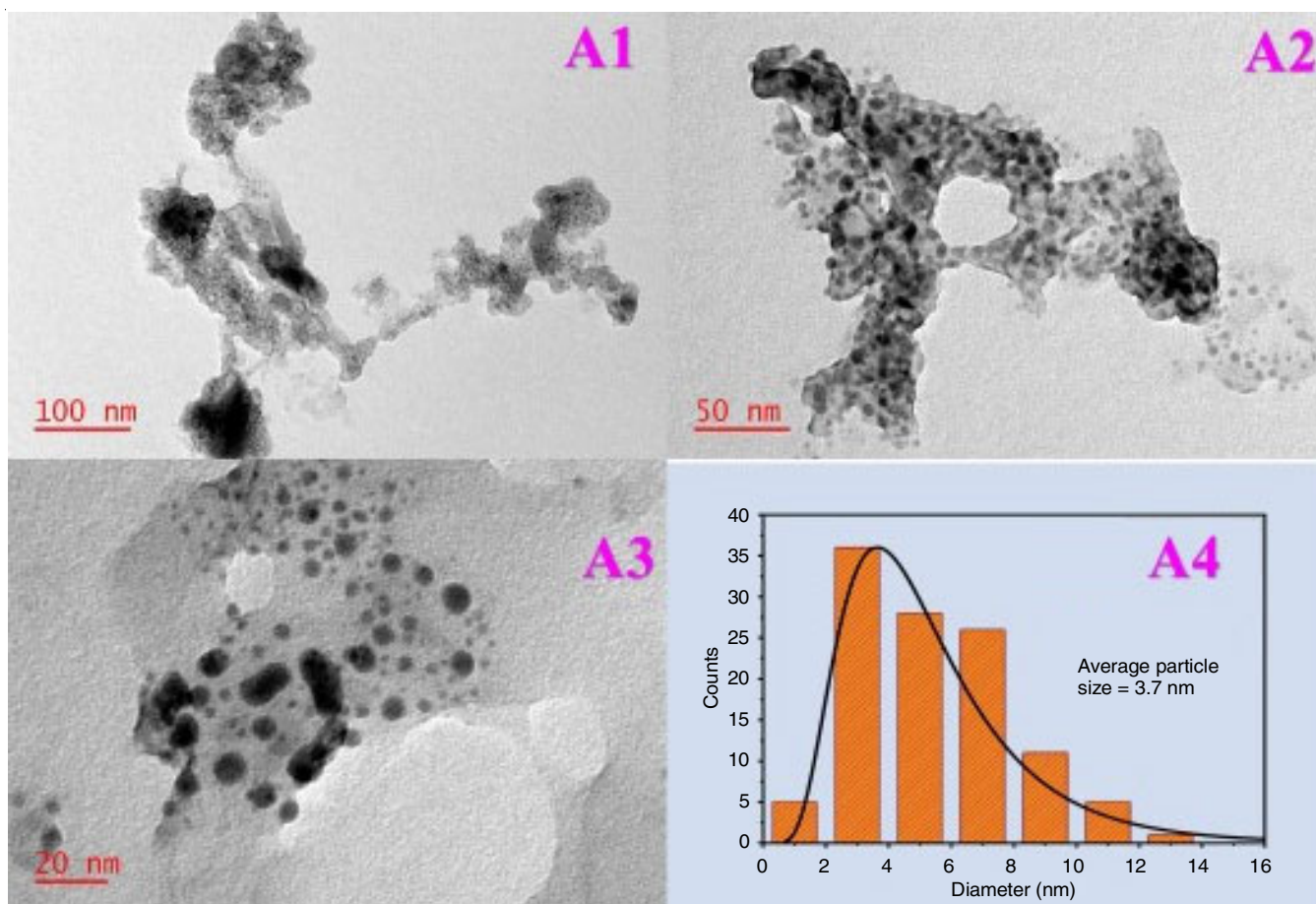
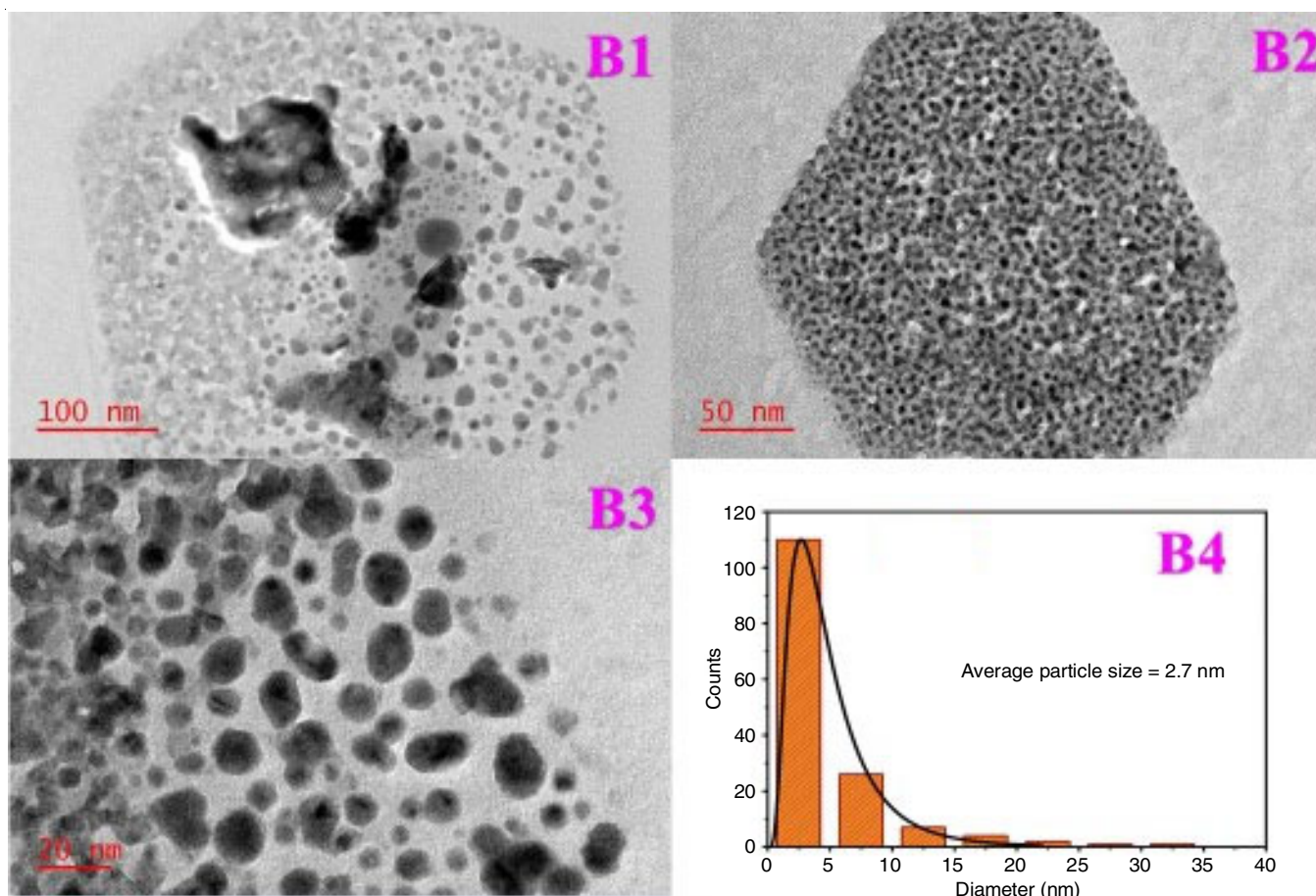Fig. 5. TEM images of sample A (A1), (A2), (A3) and the size distribution graph (A4)

Fig. 6. TEM images of sample B (B1), (B2), (B3) and the size distribution graph (B4)
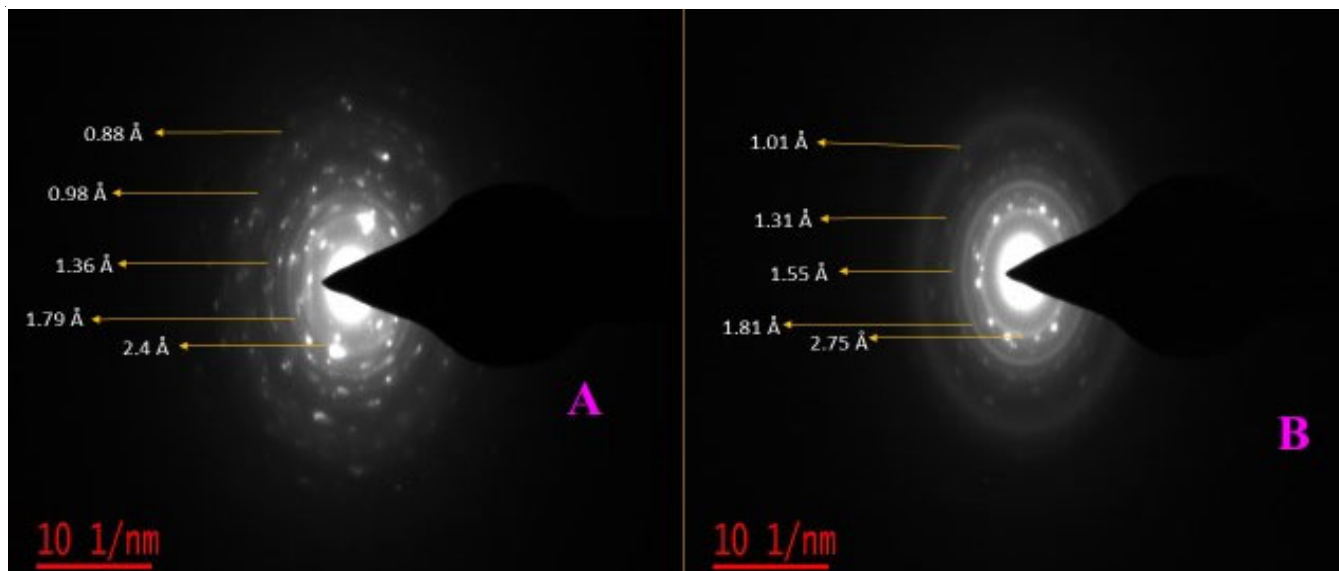

Fig. 7. SAED pattern of the sample A and B

Dr. Harisingh Gour Vishwavidyalaya Vishwavidyalaya, Sagar, India for TEM analysis.

CONFLICT OF INTEREST

The authors declare that there is no conflict of interests regarding the publication of this article.

REFERENCES

1. A.G. Al-Sehemi, A.S. Al-Shihri, A. Kalam, G. Du and T. Ahmad, *J. Mol. Struct.*, **1058**, 56 (2014);
    https://doi.org/10.1016/j.molstruc.2013.10.065
2. S. Bayda, M. Adeel, T. Tuccinardi, M. Cordani and F. Rizzolio, *Molecules*, **25**, 112 (2020);
    https://doi.org/10.3390/molecules25010112

3. R.P. Feynman, There's Plenty of Room at the Bottom - An Invitation to Enter a New Field of Physics, Engineering and Science Magazine of California Institute of Technology, vol. 23, p. 22 (1960).

4. M. Singh, S. Manikandan and A.K. Kumaraguru, *Res. J. Nanosci. Nanotechnol.*, **1**, 1 (2011);
https://doi.org/10.3923/rjnn.2011.1.11

5. J. Jeevanandam, A. Barhoum, Y.S. Chan, A. Dufresne and M.K. Danquah, *Beilstein J. Nanotechnol.*, **9**, 1050 (2018);
https://doi.org/10.3762/bjnano.9.98

6. J.H. Crabtree, R.J. Burchette, R.A. Siddiqi, I.T. Huen, L.L. Hadnott and A. Fishman, *Perit. Dial. Int.*, **23**, 368 (2003);
https://doi.org/10.1177/089686080302300410

7. A. Królikowska, A. Kudelski, A. Michota and J. Bukowska, *Surf. Sci.*, **532–535**, 227 (2003);
https://doi.org/10.1016/S0039-6028(03)00094-3

8. N. Baig, I. Kammakakam and W. Falath, *Mater. Adv.*, **2**, 1821 (2021);
https://doi.org/10.1039/D0MA00807A

9. V. Chandrakala, V. Aruna and G. Angajala, *Emergent Mater.*, (2022);
https://doi.org/10.1007/s42247-021-00335-x

10. H. Karami, M.A. Karimi, S. Haghdar, A. Sadeghi, R. Mir-Ghasemi and S. Mahdi-Khani, *Mater. Chem. Phys.*, **108**, 337 (2008);
https://doi.org/10.1016/j.matchemphys.2007.09.045

11. A. Thulasiramudu and S. Buddhudu, *Spectrochim. Acta A Mol. Biomol. Spectrosc.*, **66**, 323 (2007);
https://doi.org/10.1016/j.saa.2006.02.060

12. C. Barriga, S. Maffi, L. Peraldo Bicelli and C. Malitesta, *J. Power Sources*, **34**, 353 (1991);
https://doi.org/10.1016/0378-7753(91)80101-3

13. W.U. Huynh, J.J. Dittmer and A.P. Alivisatos, *Science*, **295**, 2425 (2002);
https://doi.org/10.1126/science.1069156

14. M.S. Sonmez and R.V. Kumar, *Hydrometallurgy*, **95**, 53 (2009);
https://doi.org/10.1016/j.hydromet.2008.04.012

15. J. Senvaitiene, J. Smirnova, A. Beganskiene and A. Kareiva, *Acta Chim. Slov.*, **54**, 185 (2007).

16. B. Jaffe, R.S. Roth and S. Marzullo, *J. Res. Natl. Bur. Stand.*, **55**, 239 (1955);
https://doi.org/10.6028/jres.055.028

17. A. Miri, M. Sarani, A. Hashemzadeh, Z. Mardani and M. Darroudi, *Green Chem. Lett. Rev.*, **11**, 567 (2018);
https://doi.org/10.1080/17518253.2018.1547926

18. G. El-Damrawi and E. Mansour, *Physica B*, **364**, 190 (2005);
https://doi.org/10.1016/j.physb.2005.04.012

19. E. Casals, S. Vazquez-Campos, N. Bastus and V. Puntes, *Trac-Trends Anal. Chem.*, **27**, 672 (2008);
https://doi.org/10.1016/j.trac.2008.06.004

20. C. McGovern, *Nanotechnol. Percept.*, **6**, 155 (2010);
https://doi.org/10.4024/N15GO10A.ntp.06.03

21. C. Stephenson and A. Hubler, *Sci. Rep.*, **5**, 15044 (2015);
https://doi.org/10.1038/srep15044

22. D. Lyon and A. Hubler, *IEEE Trans. Dielectr. Electr. Insul.*, **20**, 1467 (2013);
https://doi.org/10.1109/TDEI.2013.6571470

23. G. Valenti, E. Rampazzo, S. Bonacchi, L. Petrizza, M. Marcaccio, M. Montalti, L. Prodi and F. Paolucci, *J. Am. Chem. Soc.*, **138**, 15935 (2016);
https://doi.org/10.1021/jacs.6b08239

24. P. Keratitayanan, J.K. Carrow and A.K. Gaharwar, *Adv. Healthcare Mater.*, **4**, 1600 (2015);
https://doi.org/10.1002/adhm.201500272

25. K.C. Chen, C.W. Wang, Y.I. Lee and H.G. Liu, *Colloids Surf. A Physicochem. Eng. Asp.*, **373**, 124 (2011);
https://doi.org/10.1016/j.colsurfa.2010.10.035

26. S. Ghasemi, M.F. Mousavi, M. Shamsipur and H. Karami, *Ultrason. Sonochem.*, **15**, 448 (2008);
https://doi.org/10.1016/j.ultsonch.2007.05.006

27. L. Shi, Y. Xu and Q. Li, *Cryst. Growth Des.*, **8**, 3521 (2008);
https://doi.org/10.1021/cg700909v

28. M.M. Kashani-Motlagh and M.K. Mahmoudabad, *J. Sol-Gel Sci. Technol.*, **59**, 106 (2011);
https://doi.org/10.1007/s10971-011-2467-y

29. J.C. Schottmiller, *J. Appl. Phys.*, **37**, 3505 (1966);
https://doi.org/10.1063/1.1708890

30. M.S. Chavali and M.P. Nikolova, *SN Appl. Sci.*, **1**, 607 (2019);
https://doi.org/10.1007/s42452-019-0592-3

31. P. Makula, M. Pacia and W. Macyk, *J. Phys. Chem. Lett.*, **9**, 6814 (2018);
https://doi.org/10.1021/acs.jpclett.8b02892

32. V.N. Suryawanshi and M.D. Deshpande, *AIP Conf. Proceed.*, **2335**, 080012 (2021);
https://doi.org/10.1063/5.0046133

33. K.T. Arulmozhi and N. Mythili, *AIP Adv.*, **3**, 122122 (2013);
https://doi.org/10.1063/1.4858419